Hindawi
Journal of Electrical and Computer Engineering
Volume 2022, Article ID 7694026, 19 pages
https://doi.org/10.1155/2022/7694026

*Research Article*

# A Novel Chaotic Rao-2 Algorithm for Optimal Power Flow Solution

**Warid Warid**

*Electromechanical Systems Engineering Department, Thi-Qar Technical College, Southern Technical University, Basra, Iraq*

Correspondence should be addressed to Warid Warid; warid.sayel@stu.edu.iq

Received 29 July 2022; Revised 24 October 2022; Accepted 26 October 2022; Published 4 November 2022

Academic Editor: Yang Li



This article suggests a novel chaotic Rao-2 algorithm to solve various optimal power flow (OPF) problems. The basic Rao-2 solver is a newly developed metaphor-less optimization tool. The novel optimization course of the basic Rao-2 algorithm relies on the finest and inferior solutions within the population and the indiscriminate interrelations among the nominee individuals. This tactic allows superior directions to scrutinize the exploration space. In this work, a novel chaotic Rao-2 algorithm-inspired scheme for handling the OPF problem is offered. In the offered solver, a chaotic tactic is amalgamated into the movement formula of the basic Rao-2 algorithm to enhance the variety of solutions and enhance both its global and local search capabilities. This novel scheme, which incorporates the features of the basic Rao-2 algorithm and chaotic dynamics, is then utilized to solve various OPF problems. For the OPF solution, five situations are investigated. The offered solver is examined on two standard IEEE test grids and the emulation outcomes are evaluated with the outcomes offered in the other publications and deemed competitive in terms of the features of the solution. The offered chaotic Rao-2 algorithm outperforms the basic Rao-2 algorithm regarding convergence velocity and solution competence. Furthermore, a test is performed to validate the statistical worth of the offered chaotic Rao-2-inspired solver. The offered chaotic Rao-2 algorithm presents a vigorous and simple solution for the OPF framework under various objectives.

## 1. Introduction

Optimum analysis, observation, and control of modernistic power grid operations necessitates efficacious tools [1]. These days, optimal power flow (OPF) is the most trustworthy tool for power grid operators [2]. The OPF efficiently offers an improvement in power network operation by optimizing a definite goal function while gratifying specific constraints [2, 3]. Owing to the fact that there is a combination of continuous as well as discrete variables, the OPF problem is considered a nondifferentiable, multimodal, nonlinear, restricted optimization task [3–5]. Due to the incessant advances in computational intelligence, abundant metaheuristic optimization tactics have emanated so far and have been tested to deal with the various tricky OPF frameworks confronting electric companies. Most existing metaheuristic techniques are based on the metaphor of various natural phenomena, habitual actions of animals, and musical instruments, such as the electromagnetism-like mechanism (EM) algorithm [1], chaotic salp swarm optimization (CSSO) algorithm [2], differential search algorithm (DSA) [5], artificial bee colony (ABC) algorithm [6], group search optimization (GSO) [7], imperialist competitive algorithm (ICA) [8], tree-seed algorithm (TSA) [9], krill herd algorithm (KHA) [10], particle swarm optimization (PSO) algorithm [11], social spider optimization (SSO) algorithm [12], harmony search (HS) algorithm [13], and ant lion optimizer (ALO) [14].

These algorithms utilize evolution concepts rather than deterministic ones, do not involve gradient computation, demonstrate the good ability to not get stuck in crafty local optima, and have the merit of solving large-scale nonlinear, complicated optimization problems [5]. Regardless of their merits, many of these introduced techniques are vanishing naturally because they have no users, and some have earned attention to a certain degree [15]. Furthermore, such solvers

require suitably altered algorithm-particular controlled factors, as erroneous controlling of such factors will constrain the convergence feature or guide to a suboptimal solution. Existing metaheuristic algorithms have been used to solve complex optimization problems with good performance. Still, there is the problem of premature convergence caused by a lack of suitable harmonizing between exploration and exploitation processes [16]. Many population-based techniques offer an infeasible solution to the OPF problem in terms of violation of the state variable constraints, as reported in [17, 18]. Thus, it is essential to introduce straightforward metaphor-less algorithms to solve complicated optimization problems rather than develop metaphor-based methods.

Several studies have tackled the single OPF problem. In reference [19], an adaptive constraint differential evolution (ACDE) algorithm was offered to solve the problem of OPF. In ACDE, the crossover velocity sorting tactic and the reusing successful evolution direction technique were used to enhance the act of adaptive differential evolution. In reference [20], an improved salp swarm algorithm (ISSA) to enhance the search capability of the SSA was suggested. In reference [21], a new gorilla troop optimization technique (GTOT) was modified to solve the OPF problem. In reference [22], a recently reported metaheuristic technique known as boundary-assigned animal migration optimization (BA-AMO) has been implemented for the OPF study. This approach yielded an improved performance as compared to the basic AMO in terms of searching and reaching better minima. In reference [3], an enhanced adaptive differential evolution (JADE) with a self-adaptive penalty constraint handling technique, namely, EJADE-SP, was utilized for the OPF study. In reference [1], an improved electromagnetism-like mechanism method (IEM) was utilized for the OPF study. This algorithm gave superior performance as compared to the basic EM in terms of solution quality. In reference [4], an integrated optimization algorithm, instituted with the incorporation of the invasive weed optimization (IWO) and Powell's pattern search (PPS) technique, was introduced to solve the OPF. The IWO-PPS performed superior as compared to the IWO algorithm in terms of the solution eminence and convergence rate. In reference [7], a group search optimization algorithm (GSO) was used for the OPF. The GSO offered superior results as compared to those attained by other techniques. On the other hand, a set of recent works have been reported to solve the multiobjective OPF problem. In reference [23], a two-stage solution technique to solve the problem of MOPF for AC/DC grids using a multiobjective particle swarm optimization (MOPSO) method was suggested. In reference [24], a novel parallel bi-criterion evolution indicator based evolutionary algorithm (BCE-IBEA) algorithm was offered to solve a new corrective security-constrained MOPF method. In reference [25], a PSO algorithm with dynamic velocity control was utilized to solve the multiobjective OPF problem. Furthermore, some novel optimization algorithms have been utilized to solve both the single and multiobjective OPF problems, the estimation of the OPF framework for several single and multiobjective functions was executed in reference [26] using a new fuzzy adaptive hybrid self-adaptive PSO and differential evolution techniques, namely, FAHSPSO-DE. In reference [27], a developed Archimedes optimization algorithm (IAOA) was offered to avoid premature convergence problems in AOA. In reference [28], a differential-based harmony search algorithm (DH/best) was used to solve the single and multiobjective OPF problems. This algorithm has a superior initialization tactic and a better updating process compared to other techniques.

Recently, a straightforward metaphor-less optimization solver, namely, the Rao-2 algorithm, has been proposed by Rao [15] in 2020. The novel optimization scheme of this solver relies on the best and inferior solutions within the population and the arbitrary interactions between the candidate solutions. This tactic makes superior directions to scan the exploration space. Unlike many existing metaheuristic optimization solvers, the Rao-2 algorithm does not need any solver-particular controlling parameters. The author has scrutinized the effectiveness of the Rao-2 algorithm on 23 benchmark problems. The comparative results revealed the supremacy of the Rao-2 algorithm over numerous competitive methods. In reference [29], the basic Rao-2 algorithm was used to solve the OPF problem. However, the Rao-2 algorithm endures premature convergence problems and consequently can be entangled in local optimums. Furthermore, it requires more modifications to attain the global optimum solution in a feasible time. In reference [30], quasi-oppositional and Levy flight techniques were utilized to enhance the activity of the Rao algorithm. This article aimed to avert these obstacles and enhance the performance of the basic Rao-2 algorithm. Here, a novel chaotic Rao-2 algorithm is introduced. A mutation strategy (i.e., the chaotic dynamic) was employed in the basic Rao-2 algorithm to enhance both its global and local exploration capabilities. Chaotic dynamics were confirmed to be able to enhance the exploration capabilities of metaheuristic algorithms in terms of evading premature convergence [16, 31]. Chaotic maps have been effective in diversifying the population to a superior stage to evade the entrapment of the individuals in the local region(s) and give a better convergence rate with high accuracy [16]. The chaotic sequence offered by the logistic map is embedded into the basic Rao-2 algorithm to control the search equation. It is important to mention that the adaptations embedded in the basic Rao-2 algorithm did not influence its two fundamental traits, i.e., straightforwardness and the lack of a need for algorithm-specific controlling parameters.

To contribute to the OPF state-of-the-art, the optimization of OPF is executed for the first time in this article by the suggested novel chaotic Rao-2 algorithm for solving different single-objective OPF frameworks. The major contributions of this article can be stated as follows:

(1) a novel chaotic Rao-2 algorithm is introduced to evade the drawbacks of the basic Rao-2 algorithm.

(2) a novel chaotic Rao-2 algorithm-inspired scheme for solving the OPF problem is offered to obtain a superior solution in terms of quality and convergence rate.

(3) to handle the problem of premature convergence in the basic Rao-2 algorithm, the chaotic dynamic was amalgamated into the movement formula of the basic Rao-2 algorithm to enhance the variety of solutions and enhance both its global and local search capabilities.

(4) investigating the competence of the suggested chaotic Rao-2 algorithm on two typical IEEE test grids.

(5) implementing a comparative test between the simulation results of the suggested chaotic Rao-2 solver, the basic Rao-2 algorithm as well as other optimization techniques given in the former publications.

(6) executing a statistical test to authenticate the reliability of the suggested chaotic Rao-2 algorithm when solving different OPF frameworks.

(7) different cases of single objective OPF are studied and solved successfully by the chaotic Rao-2 tactic in this work: minimization of fuel cost, decreasing of active power losses, voltage stabilization reinforcement, voltage profile improvement, and voltage profile improvement with fuel cost reduction.

(8) unlike many other existing algorithms used to solve the OPF, an effective strategy to handle the state variable constraints is employed to maintain the solution feasibility. These constraints are incorporated into the objective function as quadratic penalty terms.

The rest of this article is organized as follows: the OPF problem is formulated in Section 2. The basic Rao-2 algorithm is succinctly explained in Section 3. In Section 4, the suggested novel chaotic Rao-2 algorithm is introduced. The novel chaotic Rao-2 algorithm-inspired scheme for handling the OPF problem is stated in Section 5. The test system, simulation results, discussions, and statistical assessment are introduced in Section 6. Also, the results achieved using the chaotic Rao-2 algorithm are compared with those obtained using different global optimization algorithms. Finally, the conclusions are given in Section 7.

## 2. OPF Formulation

The main task of OPF is to estimate the optimum settings of the power grid control variables for optimizing a chosen objective while satisfying specific grid constraints. The following mathematical expressions introduce the general formulation of the OPF problem:

$$\text{Optimize } J(X,U), \tag{1}$$

expose to

$$\begin{aligned} g(X,U) &= 0, \\ z(X,U) &\le 0, \end{aligned} \tag{2}$$

where $J$ and $g(X,U)$ state the objective and the equality constraints, correspondingly. $z(X,U)$ signifies the power system operation constraints. $U$ is the vector of control variables and $X$ is the vector of state variables.

The control vector $U$ comprises a set of system variables as follows:

(1) Tap setting of tap-changing transformers (Treg)

(2) Voltage magnitude at generation buses ($V_G$)

(3) Real power outputs of generation buses ($P_G$) except for the slack bus

(4) Shunt VAR compensation ($Q_S$)

The $U$ vector can be denoted as follows:

$$U = \left[\text{Treg}_1, \ldots, \text{Treg}_{N_T}, V_{G1}, ..., V_{GN_G}, P_{G2}, \ldots, P_{GN_G}, Q_{S1}, ..., Q_{SN_C}\right]^T, \tag{3}$$

where $N_T$, $N_g$, and $N_c$ are the number of regulating transformers, system generators, and shunt VAR compensators, respectively. The $U$ vector variables must be controlled within their authorized minimum and maximum limits as follows:

$$\text{Treg}_i^{\min} \le \text{Treg}_i \le \text{Treg}_i^{\max} \quad i = 1, 2, \ldots.., N_T, \tag{4}$$

$$V_{Gi}^{\min} \le V_{Gi} \le V_{Gi}^{\max} \quad i = 1, 2, \ldots.., N_G, \tag{5}$$

$$P_{Gi}^{\min} \le P_{Gi} \le P_{Gi}^{\max} \quad i = 2, 3, .. \ldots, N_G, \tag{6}$$

$$Q_{Si}^{\min} \le Q_{Si} \le Q_{Si}^{\max} \quad i = 1, 2, \ldots.., N_C, \tag{7}$$

The vector $X$ comprises a set of variables that express the system state as follows:

(1) The active power generation of the slack bus ($P_{G1}$)

(2) Voltage magnitude of load buses ($V_L$)

(3) The apparent power flow ($S_{Tline}$)

(4) Reactive power of generation buses ($Q_G$)

The $X$ vector can be expressed as follows:

$$X = \left[P_{G1}, V_{L1}, ..., V_{LN_L}, S_{\text{Tline},1}, ..., S_{\text{Tline},N_l}, Q_{G1}, ..., Q_{GN_G}\right]^T, \tag{8}$$

where $N_L$ and $N_l$ are the number of load buses and system lines, respectively. The $X$ vector variables have to be controlled within their authorized minimum and maximum limits as follows:

$$\begin{aligned} P_{G1}^{\min} &\le P_{G1} \le P_{G1}^{\max}, \\ V_{Li}^{\min} &\le V_{Li} \le V_{Li}^{\max} \quad i = 1, 2, \ldots.., N_L, \\ S_{T\text{line},i} &\le S_{T\text{line},i}^{\max} \quad i = 1, 2, \ldots.., N_l, \\ Q_{Gi}^{\min} &\le Q_{Gi} \le Q_{Gi}^{\max} \quad i = 1, 2, \ldots N_G. \end{aligned} \tag{9}$$

Quadratic penalty terms are merged with the objective function to consider the state variable constraints as follows:

$$J' = J + \lambda_1\left(P_{G1} - P_{G1}^{\lim}\right)^2 + \lambda_2\sum_{i=1}^{N_L}\left(V_{Li} - V_{Li}^{\lim}\right)^2 + \lambda_3\sum_{i=1}^{N_l}\left(S_{T\text{line},i} - S_{T\text{line},i}^{\max}\right)^2 + \lambda_4\left(\sum_{i=1}^{N_G} Q_{Gi} - Q_{Gi}^{\lim}\right)^2, \tag{10}$$

where $J'$ is the modified objective formulation. $\lambda_1, \lambda_2, \lambda_3$, and $\lambda_4$ are the penalty coefficients. $x^{\lim}$ is the maximum/minimum frontier value of the state variable $x$ that can be described in the following manner

$$x^{\lim} = \begin{cases} x^{\min} & x < x^{\min} \\ x^{\max} & x > x^{\max} \end{cases}. \tag{11}$$

If $x^{\min} \le x \le x^{\max}$, then the quadratic penalty term becomes zero.

## 3. Rao-2 Algorithm

The Rao-2 algorithm is one of the latest metaheuristic optimization tools, which was proposed by Rao [15] in 2020. The optimization course of this algorithm depends on the finest and inferior solutions within the population and the indiscriminate interactions between the nominee individuals. This approach creates superior directions to scrutinize the exploration space. Unlike many existing metaheuristic optimization solvers, the Rao-2 algorithm does not need any solver-particular controlling parameters and utilizes only the three standard control factors: $C$ (no. of design variables where $v = 1,2,3, \ldots., C$), $D$ (no. of candidate solutions where $k = 1,2,3, \ldots., D$), and $Gn$ (no. of iterations). The optimization phase of the Rao-2 algorithm is directed by one straightforward equation. If $u_{v,k,i}$ is the value of the $v$th control variable for the $k$th nominee individual in the course of the $i$th generation, then this value is amended as follows:

$$\begin{aligned} u'_{v,k,i} = u_{v,k,i} &+ r_{1,v,i}\left(u_{v,\text{best},i} - u_{v,\text{worst},i}\right) \\ &+ r_{2,v,i}\left(\left|u_{v,k,i} \text{or} u_{v,p,i}\right| - \left|u_{v,p,i} \text{or} u_{v,k,i}\right|\right), \end{aligned} \tag{12}$$

where $r_{1,v,i}$ and $r_{2,v,i}$ are the two random numbers for the $v$ th control variable in the course of the $i$th generation in the domain of [0, 1]. $u_{v,\text{best},i}$ and $u_{v,\text{worst},i}$ stand for the values of the $v$ th control variable for the finest and inferior candidate solutions within the population, respectively. $u'_{v,k,i}$ is the amended value of $u_{v,k,i}$. $u_{v,p,i}$ is an indiscriminately selected contender solution $p$.

The third expression in the former equation stands for the indiscriminate interactions between the nominee individuals. The expression $((u_{v,k,i} \text{or} u_{v,p,i}))$ states that the nominee solution $k$ is compared with an indiscriminately selected nominee solution $p$ in terms of the value of the objective function as follows:

If the value of the objective function for the $k$th nominee solution is superior to the value of the objective function for the $p$th nominee solution, then the term expression $((u_{v,k,i} \text{or} u_{v,p,i}))$ becomes $u_{v,k,i}$.

If the value of the objective function for the $p$th nominee solution is superior to the value of the objective function for the $k$th nominee solution, then the term expression $((u_{v,k,i} \text{or} u_{v,p,i}))$ becomes $u_{v,p,i}$.

Meanwhile, the expression $((u_{v,p,i} \text{or} u_{v,k,i}))$ states that the nominee solution $p$ is compared with an indiscriminately selected nominee solution $k$ in terms of the value of the objective function as follows:

If the value of the objective function for the $k$th nominee solution is superior to the value of the objective function for the $p$th nominee solution, then the term expression $((u_{v,p,i} \text{or} u_{v,k,i}))$ becomes $u_{v,p,i}$.

If the value of the objective function for the $p$th nominee solution is superior to the value of the objective function for the $k$th nominee solution, then the term expression $((u_{v,p,i} \text{or} u_{v,k,i}))$ becomes $u_{v,k,i}$. Figure 1 shows the flowchart of the Rao-2 algorithm.

## 4. The Suggested Chaotic Rao-2 Algorithm

A novel chaotic Rao-2 algorithm is introduced to handle the problem of premature convergence in the basic Rao-2 algorithm. In the offered solver, the chaotic dynamics are amalgamated into the movement formula of the basic Rao-2 algorithm to enhance the variety of solutions and avoid being entangled in local optima. The liberation of the entrapped individuals in the local optima is possible because of a sudden alteration in the values offered by the chaotic oscillations. In the modified movement equation of the Rao-2 algorithm, two chaotic random numbers $c_{m1}$ and $c_{m2}$ are used instead of the two random numbers $r_1$ and $r_2$, respectively, as follows:

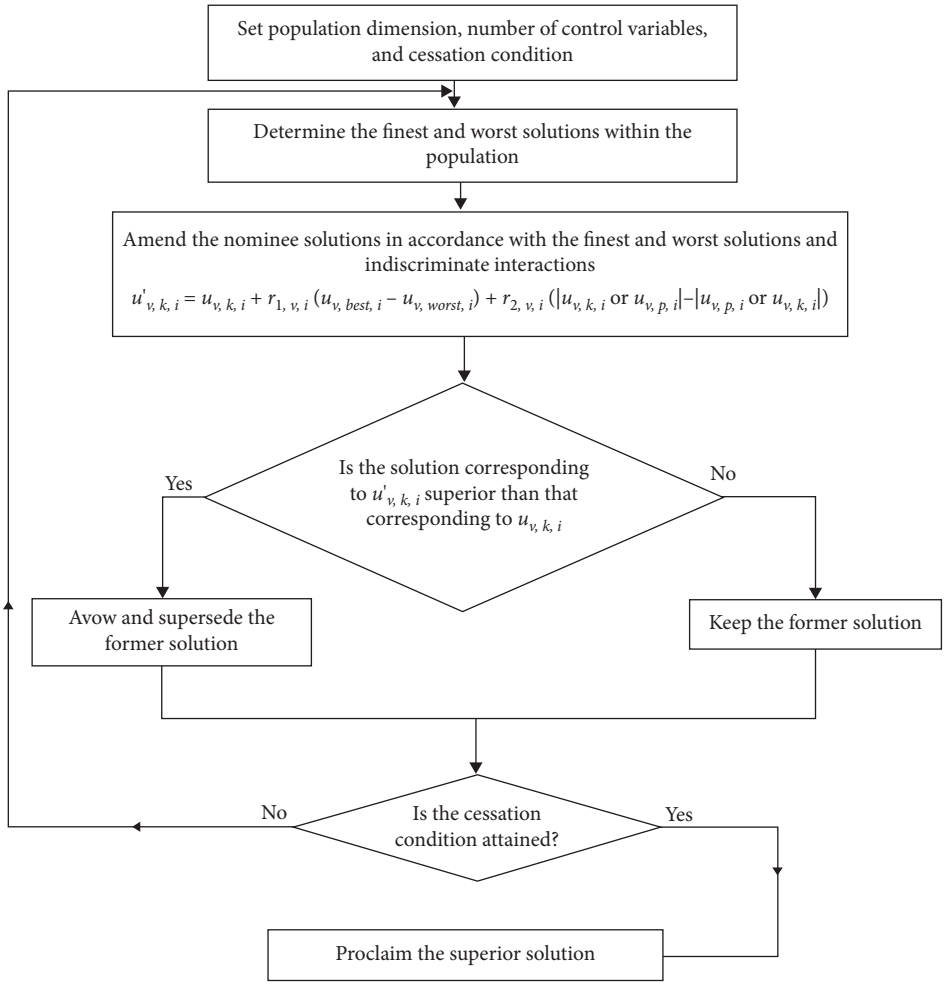


Figure 1: Flowchart of the Rao-2 algorithm [15].

$$u'_{v,k,i} = u_{v,k,i} + c_{m1,v,i}\left(u_{v,best,i} - u_{v,\text{worst},i}\right) + c_{m2,v,i}\left(\left|u_{v,k,i} \text{ or} u_{v,p,i}\right| - \left|u_{v,p,i} \text{ or} u_{v,k,i}\right|\right), \tag{13}$$

where $c_{m1,v,i}$ and $c_{m2,v,i}$ are the two chaotic numbers for the $v$ th control variable in the course of the $i$th generation. The chaotic random numbers $c_m$ (i.e., the chaotic series) utilized in this article are the logistic map stated by the following formula:

$$c_{m+1} = 4c_m(1 - c_m), \tag{14}$$

where $m$ is the iteration number and $c_m$ is the value of $m$th chaotic iteration. The initial value $c_0$ is arbitrarily formed in the range of [0, 1].

## 5. A Novel Chaotic Rao-2 Algorithm-Inspired Scheme for Handling the OPF Problem

In this section, a novel chaotic Rao-2 algorithm-inspired scheme for handling the OPF problem is introduced as follows:

*Step 1*: Read the considered electrical grid data, including the line data, generator data and load data.

*Step 2*: Read the set of decision variables given in equation (5). These controllable variables are real power of all generation units exclusive of slack generator, voltage of generation units, reactive power of shunt VAR compensators, and tap setting of tap-changing transformers.

*Step 3*: Set the minimum and maximum frontiers of the control variables ($U_{\min}$, $U_{\max}$).

*Step 4*: Set the minimum and maximum frontiers of the state variables ($X_{\min}$, $X_{\max}$).

*Step 5*: Set the parameters of Rao-2 algorithm: $C$, $D$, as well as cessation condition (i.e., $G_n$).

*Step 6*: Create an initial arbitrary population comprising a number of solution sets ($D$) as follows:

$$P = \begin{bmatrix} U_1 \\ U_2 \\ \vdots \\ U_D \end{bmatrix} = \begin{bmatrix} u_{1,1} & u_{1,2} & \cdots & u_{1,C} \\ u_{2,1} & u_{2,2} & \cdots & u_{2,C} \\ \vdots & \vdots & \vdots & \vdots \\ u_{D,1} & u_{D,2} & \cdots & u_{D,C} \end{bmatrix} \quad (15)$$

with $k = 1, 2, 3, ..., D$ and $v = 1, 2, 3, ..., C$.

The $v$ th control variable ($u_{k,y}$ $u_{k,v}$) of the $k$th candidate individual can be defined as follows:

$$u_{k,v} = u_v^{\min} + rd\left[u_v^{\max} - u_v^{\min}\right], \quad (16)$$

where $rd$ is a uniformly distributed random number within the domain of [0, 1]. $u_v^{\max}$ is the maximum limit of the $v$ th design factor. $u_v^{\min}$ is the minimum boundary of the $v$ th control factor.

*Step 7*: Solve the power flow equations for all electrified solutions. Determine the goal value that matches each solution

*Step 8*: Determine the finest as well as inferior individuals within the population according to the values of the goal function.

*Step 9*: Amend the nominee solutions in accordance with the finest and worst solutions and random interactions according to equation (13).

*Step 10*: Check the entire modified solutions, if any $u_v^{\min}/u_v^{\max}$ is contravened, subrogate the evaluated value of the $v$ th control variable with the related constraint.

*Step 11*: Solve the power flow equations for every amended individual. Determine the goal values. Incorporate the considered penalty (s) to the value of the objective each time $x^{\min}/x^{\max}$ is contravened using equation (10).

*Step 12*: For every nominee solution, check if the solution corresponding to $u'_{v,k,i}$ is superior to that corresponding to $u_{v,k,i}$. Keep the revised solution if it is better. Otherwise, maintain the former solution.

*Step 13*: Check the cessation status. If it is accomplished, cease the algorithm and report the superior individual. Else, go to Step 8.

The strategy of the implementation of the chaotic Rao-2 algorithm to tackle the OPF is illustrated in Figure 2.

## 6. Results and Discussion

To inspect the competence of the suggested chaotic Rao-2 algorithm in solving a set of single OPF cases, the algorithm is implemented in two recognized typical networks: the IEEE 30-bus test system as well as the IEEE 118-bus test system. Moreover, to validate the chaotic Rao-2 solver, the basic Rao-2 algorithm and a set of recent competitive optimization solvers are selected for comparison. The simulations of the chaotic Rao-2 algorithm and the basic Rao-2 algorithm to deal with the considered OPF formulations are separately coded using MATLAB R2018a [32] and performed on a laptop with a 3.2 GHz processor and 16 GB of RAM.

*6.1. IEEE 30-Bus Network.* The typical IEEE 30-bus network is the first power grid elected to survey the chaotic Rao-2 algorithm competence in the state of dealing with single objective OPF frameworks. The grid data were taken from reference [33]. The grid owns 41 lines, 6 generation units, 9 shunt capacitors, and 4 tap-changing transformers. The minimum and maximum load node voltages are 0.95 per unit and 1.05 per unit, correspondingly. Five cases are studied for this system. A MATLAB code for the suggested application of the chaotic Rao-2 algorithm was separately written for each case. The chaotic Rao-2 algorithm was separately accomplished 100 times for each case. The optimal value obtained from 100 runs using the chaotic Rao-2 algorithm is reported for each case. A MATLAB code of the basic Rao-2 algorithm was separately written for each case. For a fair comparison with the chaotic Rao-2 algorithm, the optimal value obtained from 100 runs using the basic Rao-2 algorithm is reported for each case. The optimal values obtained using the chaotic Rao-2 and the basic Rao-2 algorithms are reported in the following cases. Table 1 reports the OPF results obtained from 100 runs for cases 1–5 using the chaotic Rao-2 algorithm and the basic Rao-2 algorithm. The results of the control variables are given in Table 2.

*6.1.1. Case 1: Reduction of Fuel Cost.* The foremost case to study is the reduction of fuel cost. Thus, the objective function $J$ signifies the entire fuel cost of all generators and is stated as follows:

$$J = \text{Cost} = \sum_{i=1}^{N_G} f_i, \quad (17)$$

where $f_i$ symbolizes the fuel cost of the $i$th generator as follows:

$$f_i = a_i + b_i\left(P_{Gi}\right) + c_i\left(P_{Gi}\right)^2\left(\frac{\$}{h}\right), \quad (18)$$

where $a_i$, $b_i$, and $c_i$ signify the fuel cost factors of the $i$th generator, whereas $P_{Gi}$ is the real power output of the $i$th generation unit. According to equation (10), the modified objective function $J'$ can be written in the following manner.

$$J' = \text{Cost} + \text{Penalty}. \quad (19)$$

The penalty factors $\lambda_1, \lambda_2, \lambda_3$, and $\lambda_4$ are selected as 10000 to avoid the unfeasible solutions. The novel chaotic Rao-2 algorithm and the basic Rao-2 algorithm have been executed for optimizing the modified goal function $J'$. The variation of fuel cost (symbolizing the convergence attributes of the chaotic Rao-2 and Rao-2 algorithms) is illustrated in Figure 3. This figure demonstrates the good convergence speed of the chaotic Rao-2 algorithm as compared with the basic Rao-2 algorithm. The chaotic Rao-2 algorithm requires 32 iterations to converge to the optimal solution. This result shows the convergence rapidity of the suggested chaotic Rao-2 algorithm. From Table 1, the optimal fuel cost identified with the chaotic Rao-2 algorithm is 800.1537 $/h, which is superior compared to the basic Rao-2 algorithm

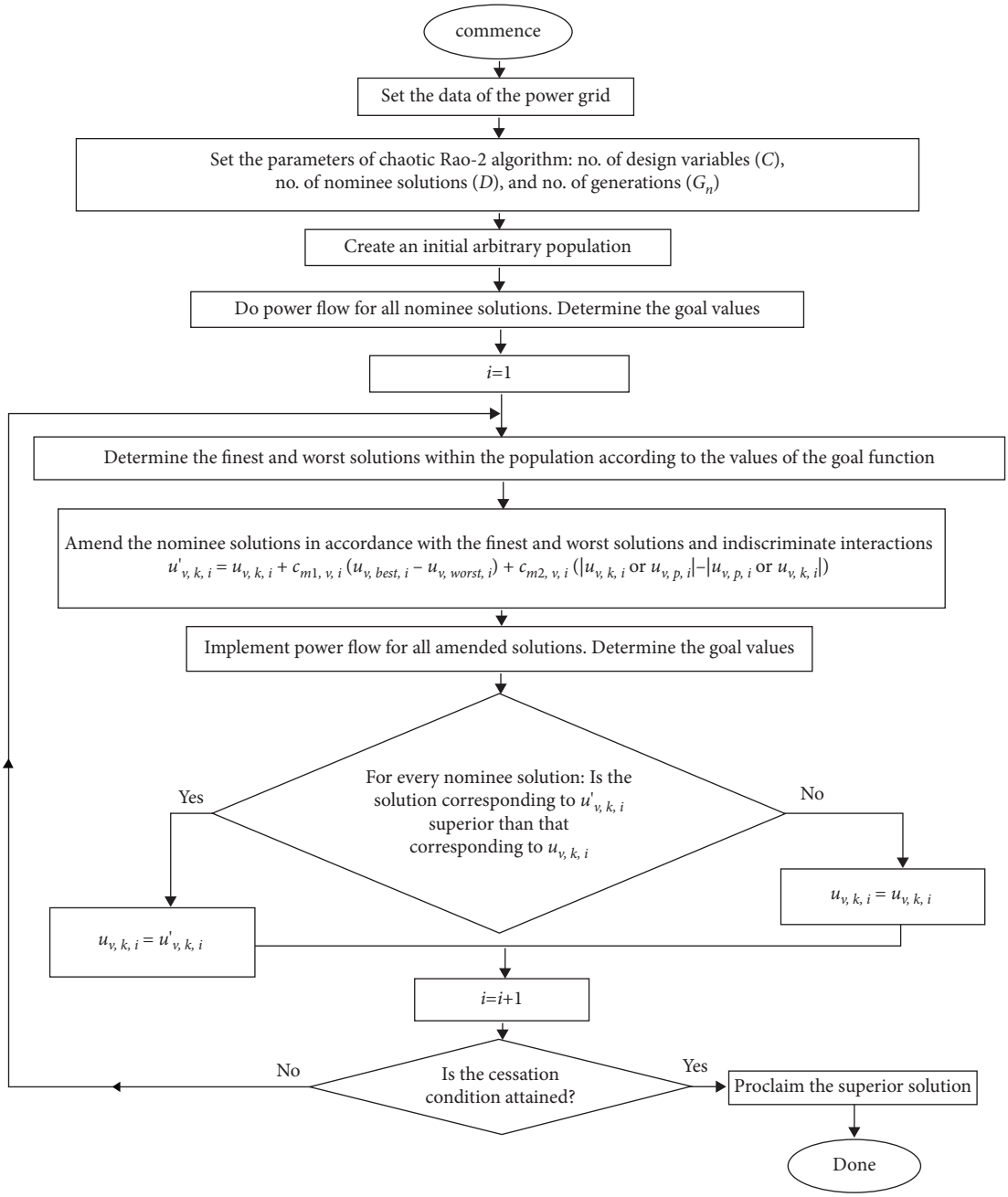


Figure 2: Flowchart of the utilization of the chaotic Rao-2 algorithm to tackle the OPF formulation.

and the former competitive optimization solvers reported in Table 3. It is obvious from Table 1 that the chaotic Rao-2 solver spends less execution time (13.503 s) than the basic Rao-2 algorithm (16.875 s). Furthermore, the chaotic Rao-2 algorithm assures that the state variable's constraints are effectively safeguarded as revealed in Table 2. It is worth mentioning that the obtained solution in FAHSPSO-DE [26], which is 799.8066 ($/h) cannot be verified because the values of all control variables are not reported. It is significant to report that many solvers utilized have contravened the feasibility frontiers, consequently yielding infeasible solutions (signified by "a"). The simulation revealed that the chaotic Rao-2 solver is a rapid-converging optimizer with excellent computational time. The chaotic Rao-2 algorithm outperforms the original Rao-2 solver regarding convergence velocity as well as solution competence. It is a competitive algorithm compared to many existing solvers reported in previous studies in terms of solution quality and validity.

*6.1.2. Case 2: Reduction of Active Power Loss.* The objective function considered is the real power loss reduction. The objective can be defined as follows:

Table 1: Simulation results for the OPF problem obtained from 100 runs for cases 1–5 using the basic Rao-2 and the chaotic Rao-2 algorithms.

| Item | *Case 1* | | *Case 2* | | *Case 3* | | *Case 4* | | *Case 5* | |
|---|---|---|---|---|---|---|---|---|---|---|
| | Chaotic Rao-2 | Rao-2 | Chaotic Rao-2 | Rao-2 | Chaotic Rao-2 | Rao-2 | Chaotic Rao-2 | Rao-2 | Chaotic Rao-2 | Rao-2 |
| PG1 | 177.2183 | 177.4346 | 51.5141 | 51.5233 | 154.51970 | 154.37656 | 104.98274 | 152.22191 | 174.49319 | 178.17728 |
| PG2 | 48.6385 | 48.6718 | 79.999915 | 80 | 34.48030 | 34.68267 | 48.362810 | 47.016624 | 50.085504 | 49.353585 |
| PG5 | 21.3935 | 21.3565 | 50 | 49.9986 | 37.18594 | 37.16101 | 50 | 44.686164 | 21.022823 | 21.973359 |
| PG8 | 21.1472 | 21.1029 | 35 | 34.9873 | 17.20649 | 17.28475 | 35 | 14.966606 | 23.319172 | 21.265377 |
| PG11 | 12.0366 | 11.8875 | 30 | 29.9999 | 12.50472 | 12.49063 | 30 | 20.629623 | 12.271069 | 10.511163 |
| PG13 | 12 | 12 | 39.994089 | 40 | 35.37582 | 35.26638 | 19.985984 | 12 | 12 | 12.154924 |
| VG1 | 1.08586 | 1.08508 | 1.06314 | 1.06257 | 1.05306 | 1.05408 | 1.0225480 | 1.0165329 | 1.0425862 | 1.0380986 |
| VG2 | 1.06629 | 1.06594 | 1.05921 | 1.05843 | 1.03867 | 1.03806 | 1.0222457 | 1.0001684 | 1.0270611 | 1.0264095 |
| VG5 | 1.03561 | 1.0341 | 1.03942 | 1.03895 | 0.99537 | 0.99604 | 1.0203167 | 1.0150936 | 1.0122406 | 1.0089113 |
| VG8 | 1.03935 | 1.03946 | 1.04541 | 1.04488 | 1.04983 | 1.05037 | 1.0118955 | 1.0089052 | 1.0076122 | 1.0057324 |
| VG11 | 1.09954 | 1.09748 | 1.09656 | 1.0804 | 1.09968 | 1.1 | 0.9933268 | 1.0815666 | 1.0397596 | 1.0744932 |
| VG13 | 1.04332 | 1.04541 | 1.0596 | 1.06405 | 1.09954 | 1.09835 | 0.9930445 | 1.0222389 | 0.9925991 | 0.9871240 |
| QC10 | 4.2960820 | 4.9432025 | 1.2868321 | 5 | 4.96315 | 5 | 5 | 4.5427378 | 4.8269723 | 5 |
| QC12 | 5 | 4.7369443 | 0 | 0 | 5 | 5 | 4.2499666 | 2.7013885 | 0 | 5 |
| QC15 | 4.3710110 | 3.6235585 | 4.3124851 | 4.93205 | 4.83057 | 4.92148 | 4.4146528 | 0 | 4.5883998 | 5 |
| QC17 | 4.9946649 | 4.9686419 | 5 | 4.93684 | 4.93516 | 4.59684 | 0 | 0 | 0.2796082 | 0.0260847 |
| QC20 | 3.5295760 | 3.6718862 | 4.4744868 | 3.81783 | 4.82535 | 5 | 5 | 4.9694913 | 5 | 5 |
| QC21 | 4.9986735 | 4.9261690 | 4.9818134 | 4.81356 | 4.85305 | 4.98047 | 4.5797353 | 3.4776893 | 4.9994249 | 5 |
| QC23 | 3.3223836 | 4.7167140 | 3.2245977 | 2.76663 | 5 | 4.97265 | 5 | 4.9968795 | 5 | 5 |
| QC24 | 4.9656267 | 4.9611172 | 5 | 5 | 4.96036 | 5 | 4.7766748 | 5 | 5 | 4.9822562 |
| QC29 | 3.0540261 | 2.4135304 | 2.5811247 | 2.69791 | 5 | 4.61073 | 4.5274734 | 3.0619722 | 2.6914685 | 2.1781773 |
| T6,9 | 1.1 | 1.0997052 | 1.1 | 1.07374 | 1.08384 | 1.08306 | 0.9997491 | 1.1 | 1.0577316 | 1.0999003 |
| T6,10 | 0.9 | 0.9 | 0.9 | 0.91126 | 0.90036 | 0.90047 | 0.9080701 | 0.9 | 0.9020170 | 0.9000287 |
| T4, 12 | 0.9720476 | 0.9753570 | 0.9964757 | 1.00559 | 1.09983 | 1.09973 | 0.9567969 | 0.9800881 | 0.9449670 | 0.9508356 |
| T28, 27 | 0.9756057 | 0.9733755 | 0.9753372 | 0.97506 | 0.98264 | 0.98285 | 0.9744802 | 0.9673128 | 0.9680990 | 0.9655151 |
| Cost ($/h) | 800.1537 | 800.3865 | 967.66625 | 967.65998 | 840.55967 | 840.27007 | 889.52282 | 844.42847 | 803.7384 | 803.81043 |
| VD | 0.8981 | 0.9056 | 0.8938 | 0.9033 | 0.9576 | 0.9509 | 0.0940385 | 0.103614 | 0.09435 | 0.0970462 |
| Loss (MW) | 9.034455 | 9.0535853 | 3.0614 | 3.0975 | 7.87297 | 7.862 | 4.9402625 | 8.1209366 | 9.7917672 | 10.035699 |
| $L_{\max}$ | 0.1263367 | 0.1264155 | 0.1275447 | 0.12694 | 0.12394 | 0.1243 | 0.135523 | 0.1367273 | 0.1367101 | 0.1362592 |
| CT (s) | 13.503 | 16.875 | 14.807 | 17.364 | 14.785 | 16.803 | 14.307 | 15.784 | 14.914 | 15.863 |
| No. of iterations | 32 | 43 | 34 | 47 | 38 | 52 | 35 | 48 | 42 | 53 |

The outcomes in intelligible form state optimum solutions obtained from 100 runs using the chaotic Rao-2 algorithm and the basic Rao-2 algorithm; $P_G$ (MW); $V_G$ (p.u.); $Q_C$ (Mvar).

$$J' = \sum_{i=1}^{N_B} P_{Gi} - \sum_{i=1}^{N_B} P_{Di} + \text{Penalty}, \tag{20}$$

where $P_{Di}$ is the real power demand at $s$th bus, whereas $N_B$ is the number of system buses. The novel chaotic Rao-2 algorithm and the basic Rao-2 algorithm have been executed for optimizing the modified objective function $J'$. The variation of real power loss (designating the convergence features of the chaotic Rao-2 algorithm and the basic Rao-2 algorithm) is elucidated in Figure 4. Figure 4 ratifies the speedy convergence rate of the chaotic Rao-2 solver. The chaotic Rao-2 algorithm requires 34 iterations to achieve the optimum solution. Once again, the chaotic Rao-2 algorithm is superior compared with the basic Rao-2 algorithm in terms of convergence speed. On the other hand, a competitive value (that is, 3.0614 MW) is recognized using the chaotic Rao-2 algorithm compared to the basic Rao-2 algorithm and the former optimization methods reported in Table 4. It is clear from Table 1 that the chaotic Rao-2 solver spends less execution time (14.807 s) than the basic Rao-2 algorithm (17.364 s). The optimization results reveal the superiority of the chaotic Rao-2 algorithm as compared to the basic Rao-2 algorithm with regard to solution quality. Remarkably, the chaotic Rao-2 algorithm ensures that the state variables' constraints are respected, as confirmed in Table 2. Once more, several algorithms used have encroached the feasibility limits, causing infeasible solutions (signified by "a") as reported in Table 4.

*6.1.3. Case 3: Voltage Stabilization Strengthening.* The third objective function considered is voltage stability enhancement. The objective can be defined as follows:

$$J' = L_{\max} + \text{Penalty}, \tag{21}$$

where $L_{\max}$ is the global voltage stability index which signifies the closeness of the system to voltage collapse. It changes from 0 to 1, corresponding to no load and voltage collapse, correspondingly. This index can be expressed as follows:

Table 2: Results of state variables.

| Variable | *Limits* | | *Case 1* | | *Case 2* | | *Case 3* | | *Case 4* | | *Case 5* | |
|---|---|---|---|---|---|---|---|---|---|---|---|---|
| | Min | Max | Chaotic Rao-2 | Rao-2 | Chaotic Rao-2 | Rao-2 | Chaotic Rao-2 | Rao-2 | Chaotic Rao-2 | Rao-2 | Chaotic Rao-2 | Rao-2 |
| QG1 | −20 | 200 | 10.0200093043973 | 8.68591978985762 | 0.409901340769281 | 0.440734482171834 | −13.5505 | −10.1342 | −18.0445 | −3.13629 | 1.47697168033147 | −8.58833 |
| QG2 | −20 | 100 | 29.99246 | 30.94129 | 18.58082 | 17.54521 | 9.495756 | 4.8926 | 38.17960 | −17.616 | 30.81213 | 37.92288 |
| QG5 | −15 | 80 | 30.62248 | 29.30512 | 25.87662 | 26.31971 | −1.86695 | −0.9973 | 48.21074 | 55.778 | 47.63780 | 43.55807 |
| QG8 | −15 | 60 | 31.39614 | 32.15187 | 31.12373 | 32.36288 | 58.38577 | 59.4008 | 58.71069 | 55.26583 | 49.70153 | 42.06078 |
| QG11 (Mvar) | −10 | 50 | 34.93810 | 33.90088 | 34.43952 | 24.38148 | 32.00848 | 32.0102 | −3.2864 | 41.81644 | 19.94781 | 38.53358 |
| QG13 (Mvar) | −15 | 60 | −4.78064 | −3.36606 | 8.340389 | 11.69406 | 39.93634 | 39.3475 | −10.5728 | 7.742227 | −11.5091 | −14.9678 |
| VL3 | 0.95 | 1.05 | 1.050190 | 1.050213 | 1.049979 | 1.050037 | 1.049728 | 1.049993 | 1.003574 | 1.000783 | 1.007276 | 1.007009 |
| VL4 | 0.95 | 1.05 | 1.042586 | 1.042779 | 1.047323 | 1.047510 | 1.048923 | 1.049028 | 0.999565 | 0.997464 | 0.999838 | 1.000481 |
| VL6 | 0.95 | 1.05 | 1.040517 | 1.040416 | 1.045357 | 1.044381 | 1.041947 | 1.042154 | 1.001841 | 1.002296 | 1.002109 | 1.003229 |
| VL7 | 0.95 | 1.05 | 1.030051 | 1.029368 | 1.034426 | 1.033652 | 1.014152 | 1.014553 | 1.000615 | 0.998668 | 0.997515 | 0.996798 |
| VL9 | 0.95 | 1.05 | 1.033705 | 1.033475 | 1.032808 | 1.035074 | 1.039406 | 1.039739 | 1.002179 | 1.001933 | 1.000156 | 1.000107 |
| VL10 | 0.95 | 1.05 | 1.046260 | 1.046793 | 1.044172 | 1.045586 | 1.049536 | 1.049589 | 1.008768 | 1.009114 | 1.008169 | 1.008331 |
| VL12 | 0.95 | 1.05 | 1.049862 | 1.050048 | 1.049918 | 1.049990 | 1.049657 | 1.049159 | 1.008344 | 1.011769 | 1.008974 | 1.008499 |
| VL14 | 0.95 | 1.05 | 1.039801 | 1.040127 | 1.039903 | 1.040155 | 1.041129 | 1.040734 | 0.999055 | 1.000274 | 0.999711 | 0.999515 |
| VL15 | 0.95 | 1.05 | 1.039429 | 1.039878 | 1.038869 | 1.039291 | 1.041212 | 1.040918 | 0.999872 | 0.999224 | 1.000390 | 1.000391 |
| VL16 | 0.95 | 1.05 | 1.042772 | 1.043096 | 1.041685 | 1.042301 | 1.043626 | 1.043243 | 1.001032 | 1.003188 | 1.001155 | 1.000829 |
| VL17 | 0.95 | 1.05 | 1.042704 | 1.043160 | 1.040851 | 1.041991 | 1.045113 | 1.044843 | 1.000911 | 1.001813 | 1.000668 | 1.000525 |
| VL18 | 0.95 | 1.05 | 1.032236 | 1.032820 | 1.031751 | 1.032065 | 1.035399 | 1.035348 | 0.994115 | 0.993787 | 0.994223 | 0.994276 |
| VL19 | 0.95 | 1.05 | 1.031099 | 1.031761 | 1.030685 | 1.030932 | 1.035114 | 1.035208 | 0.993945 | 0.993810 | 0.993819 | 0.993906 |
| VL20 | 0.95 | 1.05 | 1.035874 | 1.036574 | 1.035497 | 1.035708 | 1.040315 | 1.040485 | 0.999434 | 0.999401 | 0.999184 | 0.999287 |
| VL21 | 0.95 | 1.05 | 1.037667 | 1.038291 | 1.035703 | 1.036907 | 1.040956 | 1.041013 | 0.999844 | 0.999692 | 0.999546 | 0.99972 |
| VL22 | 0.95 | 1.05 | 1.038245 | 1.038912 | 1.036330 | 1.0375 | 1.041562 | 1.041592 | 1.000539 | 1.000492 | 1.000242 | 1.000419 |
| VL23 | 0.95 | 1.05 | 1.036198 | 1.038500 | 1.035089 | 1.035084 | 1.040598 | 1.040307 | 0.999493 | 0.999306 | 0.999952 | 1.000068 |
| VL24 | 0.95 | 1.05 | 1.031610 | 1.032775 | 1.030155 | 1.03077 | 1.035326 | 1.035108 | 0.994194 | 0.994621 | 0.994581 | 0.994856 |
| VL25 | 0.95 | 1.05 | 1.036168 | 1.036853 | 1.034735 | 1.035094 | 1.039078 | 1.038384 | 1.000278 | 1.001462 | 1.00071 | 1.001339 |
| VL26 | 0.95 | 1.05 | 1.018825 | 1.019521 | 1.017366 | 1.017732 | 1.021785 | 1.021079 | 0.982290 | 0.983494 | 0.982727 | 0.983368 |
| VL27 | 0.95 | 1.05 | 1.047431 | 1.047805 | 1.046237 | 1.046433 | 1.049923 | 1.048936 | 1.012912 | 1.014491 | 1.013266 | 1.014100 |
| VL28 | 0.95 | 1.05 | 1.035882 | 1.035611 | 1.040610 | 1.039822 | 1.040314 | 1.040491 | 0.99996 | 0.998910 | 0.998403 | 0.998552 |
| VL29 | 0.95 | 1.05 | 1.036924 | 1.035466 | 1.034359 | 1.034893 | 1.044968 | 1.042874 | 1.006334 | 1.003609 | 1.001271 | 1.000592 |
| VL30 | 0.95 | 1.05 | 1.022026 | 1.021347 | 1.020015 | 1.02041 | 1.027780 | 1.026133 | 0.989067 | 0.988182 | 0.986285 | 0.986261 |

$Q_G$ (Mvar); $V_L$ (p.u.).

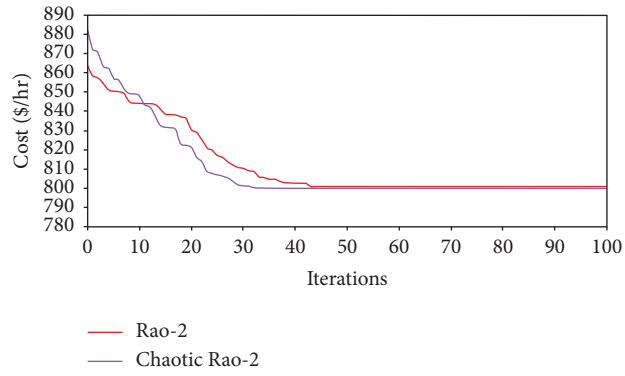


Figure 3: Convergence graphs obtained for case 1 using Rao-2 and the chaotic Rao-2 algorithms.

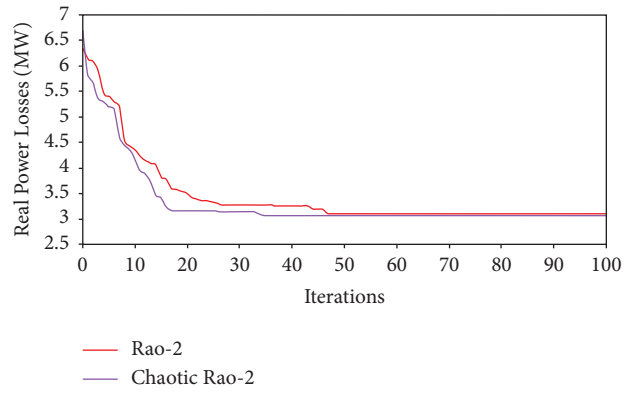


Figure 4: Convergence traits for case 2 using Rao-2 and the chaotic Rao-2 algorithms.

$$L_{\max} = \max[L_k], \quad k = 1, 2, \ldots, N_L, \tag{22}$$

where $L_k$ is the $L$-index of the $k$th load bus. The lesser the $L_{\max}$ is in a system, the more stable the system is. Hence, the reduction of $L_{\max}$ improves the voltage stability of the entire system. The novel chaotic Rao-2 algorithm and the basic Rao-2 algorithm have been implemented for optimizing the modified objective function $J'$. The convergence traits attained from the suggested chaotic Rao-2 algorithm and the basic Rao-2 algorithm for $L_{\max}$ reduction are depicted in Figure 5. The chaotic Rao-2 algorithm requires 38 iterations to discover the global solution. From Table 1, it can be noted that the optimal $L_{\max}$ recognized with the chaotic Rao-2 solver is 0.12394. It is a competitive value when compared to the basic Rao-2 algorithm and the former optimization methods reported in Table 5. It is clear from Table 1 that the chaotic Rao-2 solver spends less execution time (14.785 s) than the basic Rao-2 algorithm (16.803 s). Once more, the chaotic Rao-2 solver guarantees that the state variable constraints are successfully maintained as disclosed in Table 2.

*6.1.4. Case 4: Voltage Profile Improvement.* The fourth objective function considered is voltage profile improvement (i.e., reduction of voltage deviations). This objective can be exemplified by the voltage deviation ($VD$) of load buses from unity 1 as described in the following expression:

$$J = VD = \sum_{i=1}^{N_L} |V_i - 1|. \tag{23}$$

According to equation (14), the modified objective function $J'$ can be written in the following manner:

$$J' = VD + \text{Penalty}. \tag{24}$$

The novel chaotic Rao-2 algorithm and the basic Rao-2 algorithm have been implemented for optimizing the modified objective function $J'$. The convergence traits attained from the chaotic Rao-2 algorithm and the basic Rao-2 algorithm for $VD$ reduction are depicted in Figure 6. The chaotic Rao-2 algorithm requires 35 iterations to discover the global solution. From Table 1, the optimum $VD$ recognized with the chaotic Rao-2 solver is 0.0940385. It is a competitive value when compared to the basic Rao-2 algorithm and the former optimization algorithms reported in Table 6. Figure 7 shows a comparison of the system voltage profile obtained using the chaotic Rao-2 and Rao-2 algorithms. It can be seen that the voltage profile using the chaotic Rao-2 algorithm is enhanced compared to that of the

Table 3: Comparison study for case 1.

| Method | Cost ($/h) | VD | $P_{\text{loss}}$ (MW) | $L_{\max}$ |
|---|---|---|---|---|
| IWO-PPS [4] | 800.92 | NR | 8.017 | NR |
| PSO-SSO [34] | 798.98[a] | 1.83 | 8.602 | 0.128 |
| EJADE-SP [3] | 782.2426[a] | NR | NR | NR |
| CSSO [2] | 798.9324[a] | 1.9738 | 8.5902 | 0.1262 |
| DSA [5] | 800.3887 | NR | 8.9819 | 0.12624 |
| MSCA [17] | 799.31[a] | 1.4246 | 8.7327 | NR |
| ABCGLN [6] | 800.4464 | NR | NR | NR |
| IEM [1] | 799.1821[a] | 1.7698 | 8.6591 | 0.1176 |
| FPSO [35] | 800.72 | NR | NR | NR |
| FBICLPSO [11] | 800.0460[a] | NR | NR | NR |
| NISSO [12] | 798.9936[a] | NR | NR | NR |
| FHSA [13] | 799.914[a] | NR | NR | NR |
| DE-HS [36] | 799.0514[a] | NR | 8.613 | 0.1109 |
| PSO-APO [37] | 801.708 | NR | NR | NR |
| ICBO [38] | 799.0353[a] | 1.9652 | 8.6132 | 0.1261 |
| ARCBBO [39] | 800.5159 | 0.8867 | 9.0255 | 0.1385 |
| SF-DE [40] | 800.4131 | 0.92097 | 9.0104 | 0.13786 |
| TLBO [41] | 799.0715[a] | 1.8925 | 8.6260 | 0.1159 |
| DE [42] | 799.2891[a] | 1.5306 | 8.615 | 0.1226 |
| ABC [18] | 800.66 | 0.9209 | 9.0328 | 0.1381 |
| AGAPOP [43] | 799.8441[a] | 0.8043 | 8.9166 | NR |
| GSA [44] | 798.675143[a] | 0.872862 | 8.386049 | 0.130759 |
| FAHSPSO-DE [26] | 799.8066 | NR | NR | NR |
| ACDE [19] | 800.41132 | 0.922786 | 9.004473 | 0.137789 |
| IAOA [27] | 799.068[a] | NR | 8.62 | NR |
| ISSA [20] | 800.4752 | 0.8965 | 9.1044 | 0.1279 |
| GTOT [21] | 799.0831 | NR | 8.6263 | NR |
| Rao-2 | 800.3865 | 0.9056 | 9.0535853 | 0.1264155 |
| Chaotic Rao-2 | 800.1537 | 0.8981 | 9.034455 | 0.1263367 |

The outcomes in intelligible form state optimum; [a]infeasible result; NR, not reported.

Table 4: Comparison study for case 2.

| Solver | $P_{loss}$ (MW) | Cost ($/h) | VD | $L_{max}$ |
|---|---|---|---|---|
| PSO-SSO [34] | 2.858[a] | 965.89 | 1.91 | 0.128 |
| CSSO [2] | 2.86108[a] | 966.2214 | 1.9221 | 0.1272 |
| DSA [5] | 3.09450 | 967.6493 | NR | 0.12604 |
| MSCA [17] | 2.9334[a] | 965.6476 | 1.5987 | NR |
| IEM [1] | 2.8699[a] | 967.1147 | 1.983 | 0.1156 |
| NISSO [12] | 2.8678[a] | NR | NR | NR |
| DE-HS [36] | 3.0542[a] | 959.6311 | NR | 0.1049 |
| ABC [18] | 3.1078 | 967.681 | 0.9008 | 0.1386 |
| MSA [45] | 3.1005 | 967.6636 | 0.88868 | 0.13858 |
| ARCBBO [39] | 3.1009 | 967.6605 | 0.8913 | 0.1386 |
| SP-DE [40] | 3.0844 | 967.5962 | 0.90359 | 0.13832 |
| EGA-DQLF [46] | 3.2008 | 967.86 | NR | 0.12178 |
| ACDE [19] | 3.084041 | 967.62435 | 0.901717 | 0.138311 |
| IAOA [27] | 2.85 | 984.5599 | NR | NR |
| GTOT [21] | 2.8525 | 967.0722 | NR | NR |
| Rao-2 | 3.0975 | 967.65998 | 0.9033 | 0.12694 |
| Chaotic Rao-2 | 3.0614 | 967.66625 | 0.8938 | 0.1275447 |

The outcomes in intelligible form state optimum; aInfeasible solution; NR, not reported.

Table 5: Comparison study for case 3.

| Solver | $L_{max}$ | $P_{loss}$ (MW) | VD | Cost ($/h) |
|---|---|---|---|---|
| PSO-SSO [34] | 0.124 | 7.72 | 1.98 | 829.82 |
| CSSO [2] | 0.1241 | 7.1309 | 1.9634 | 831.2364 |
| DSA [5] | 0.1244 | 3.4217 | NR | 967.4718 |
| NISSO [12] | 0.12547 | NR | NR | NR |
| DE-HS [36] | 0.0854[a] | 5.8264 | NR | 849.6214 |
| ARCBBO [39] | 0.1369 | 9.2290 | 0.8521 | 801.8076 |
| ECHT-DE [40] | 0.13632 | 4.5224 | 0.9110 | 917.5916 |
| ACDE [19] | 0.136447 | 3.994983 | 0.911914 | 919.70514 |
| Rao-2 | 0.1243 | 7.862 | 0.9509 | 840.27007 |
| Chaotic Rao-2 | 0.12394 | 7.87297 | 0.9576 | 840.55967 |

The outcomes in intelligible form state optimum; [a]infeasible solution; NR, not reported.

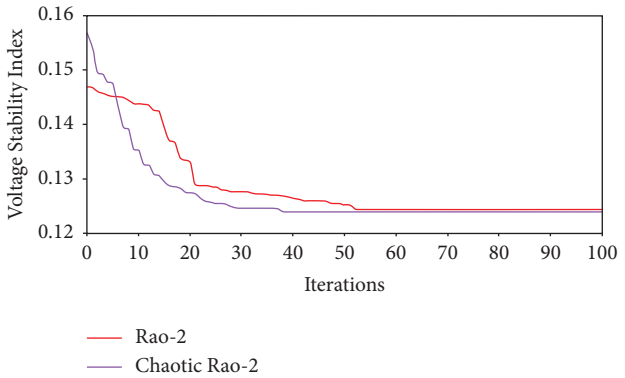


Figure 5: Convergence traits for case 3 using Rao-2 and the chaotic Rao-2 algorithms.

Rao-2 algorithm. It is noted in Table 1 that the chaotic Rao-2 solver spends less execution time (14.307 s) than the basic Rao-2 algorithm (15.784 s).

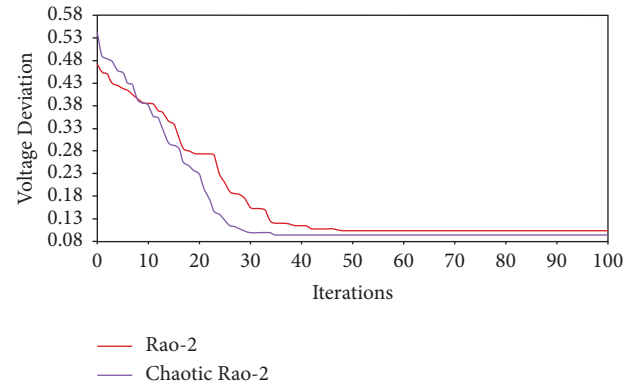


Figure 6: Convergence traits for case 4 using Rao-2 and the chaotic Rao-2 algorithms.

Table 6: Comparison study for case 4.

| Solver | VD | Cost ($/h) | $P_{loss}$ (MW) | $L_{max}$ |
|---|---|---|---|---|
| BBO [47] | 0.0951 | 805.7582 | 10.18 | NR |
| AGAPOP [43] | 0.1207 | 805.8096 | 10.6097 | NR |
| ABPPO [48] | 0.0887[a] | 871.6165 | 5.815 | 0.1367 |
| NISSO [12] | 0.09071[a] | NR | NR | NR |
| PSO-SSO [34] | 1.24 | 830.04 | 10.34 | 0.136 |
| MSCA [17] | 0.1030 | 849.281 | 7.0828 | NR |
| CSSO [2] | 0.09343[a] | 935.2189 | 11.5405 | 0.1496 |
| ACDE [19] | 0.085636 | 950.38033 | 4.075012 | 0.14888 |
| Rao-2 | 0.103614 | 844.42847 | 8.1209366 | 0.1367273 |
| Chaotic Rao-2 | 0.0940385 | 889.52282 | 4.9402625 | 0.135523 |

The outcomes in intelligible form state optimum; [a]infeasible solution; NR, not reported.

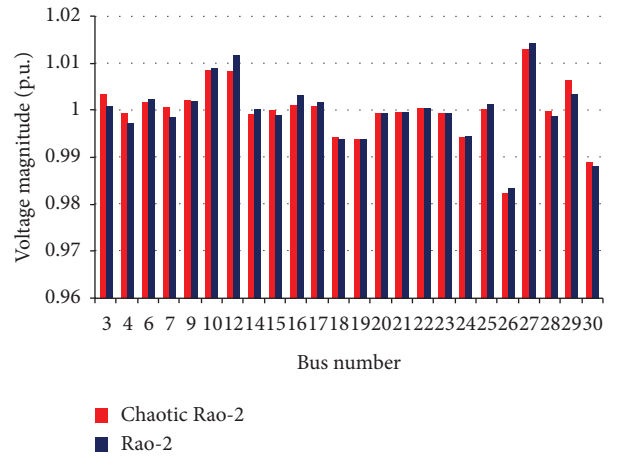


Figure 7: Comparison of system voltage profile obtained for case 4 using the chaotic Rao-2 and Rao-2 algorithms.

*6.1.5. Case 5: Voltage Profile Improvement with Cost Reduction.* The fifth objective considered is voltage profile improvement with cost reduction. This objective can be written in the following manner:

$$J' = \sum_{i=1}^{N_G} f_i + w \sum_{i=1}^{N_L} |V_i - 1| + \text{Penalty}, \quad (25)$$

Table 7: Comparison study for case 5.

| Solver | VD | Cost ($/h) | $P_{loss}$ (MW) | $L_{max}$ |
|---|---|---|---|---|
| ABPPO [48] | 0.09232 | 804.7339 | 10.072 | 0.13648 |
| DE [42] | 0.1357 | 805.2619 | 0.1316 | 10.4412 |
| TLBO [41] | 0.0945 | 803.7871 | 9.8641 | 0.1369 |
| BBO [47] | 0.102 | 804.9982 | 9.95 | NR |
| ARCBBO [39] | 0.0920 | 806.3264 | 9.6231 | 0.1490 |
| GSA [44] | 0.093269 | 804.314844 | 9.765939 | 0.135776 |
| IEM [1] | 0.1063 | 804.1084 | 9.9423 | 0.1371 |
| ICBO [38] | 0.1014 | 803.3978 | 9.7453 | 0.1490 |
| ECHT-DE [40] | 0.09454 | 803.7198 | 9.8414 | 0.14888 |
| IAOA [27] | 0.0953 | 803.57 | 9.75 | NR |
| Rao-2 | 0.0970462 | 803.81043 | 10.035699 | 0.1362592 |
| Chaotic Rao-2 | 0.09435 | 803.7384 | 9.7917672 | 0.1367101 |

The outcomes in intelligible form state optimum; [a]infeasible solution; NR, not reported.

where $w$ is a reasonable weighting parameter that should be chosen correctly to confer a weight or a significance to each one of the two expressions of the objective function. In this article, $w$ is elected as 100. The novel chaotic Rao-2 algorithm and the basic Rao-2 algorithm have been implemented for optimizing the modified objective function $J'$. The chaotic Rao-2 algorithm requires 42 iterations to achieve the optimum solution. From Table 1, the optimal $V\ D$ and fuel cost identified with the chaotic Rao-2 algorithm are 0.09435 and 803.7384 $/h, respectively, which are superior compared to the basic Rao-2 algorithm and the former competitive optimization solvers reported in Table 7. It is confirmed in Table 1 that the chaotic Rao-2 solver spends less execution time (14.914 s) than the basic Rao-2 algorithm (15.863 s). Figure 8 shows a comparison of the system voltage profile obtained for Case 1 and Case 5 using the chaotic Rao-2 algorithm. It can be seen that the voltage profile is significantly enhanced compared to that of Case 1. It decreased from 0.8981 p.u. in Case 1 to 0.09435 p.u., corresponding to minimization of 89.49% in Case 5.

*6.1.6. Robustness Investigation.* A statistical study has been implemented to conjecture the robustness of the chaotic Rao-2 algorithm. For each case study, the chaotic Rao-2 algorithm and the basic Rao-2 algorithm were separately accomplished 100 times with arbitrary initiatory populations. Four statistical test signs are considered. The obtained optimal, inferior, mean, as well as standard deviation ($SD$) quantities via the chaotic Rao-2 solver and the basic Rao-2 algorithm, are given in Table 8. It is obvious for all considered cases that the optimal, inferior, as well as mean quantities for the elected aims after 100 runs of the chaotic Rao-2 algorithm are very near, that is why the standard deviation quantities are small. The outcomes of the statistical study affirm the sturdiness of the chaotic Rao-2 algorithm in terms of discovering the optimal value in every test. The statistical study reveals that the chaotic Rao-2 algorithm is more reliable than the basic Rao-2 algorithm for all studied cases.

*6.2. IEEE 118-Bus Grid.* The IEEE 118-bus examination network is a power grid selected to scrutinize the scalability as well as the trustworthiness of the chaotic Rao-2 solver when solving enormous-range OPF formulations. The network factors are taken from reference [49]. The network has 186 transmission lines, 54 generation units, 64 load buses, 12 capacitors, and 9 controlling transformers. The minimum and maximum voltage levels of all nodes are located in the range of [0.95 and 1.1]. The imaginary power given by every capacitor is set in the range of [0 MVAR to 30 MVAR]. The minimum and maximum constraints for each controlling transformer tap are designated in the domain of [0.9, 1.1].

*6.2.1. Case 6: Reduction of Fuel Cost.* Fuel cost reduction is as elected the goal to be achieved using the chaotic Rao-2 solver. Figure 9 exemplifies the convergence trait achieved for this test. Figure 9 illustrates the advancement of the goal over iterations. The chaotic Rao-2 algorithm requires 83 iterations to get the optimum value, which reveals the good convergence rate of the chaotic Rao-2 algorithm when managing such a large-scale OPF formulation. The optimal outcome achieved is given in Table 9. The fuel cost is 129,385.643 $/h. Table 10 shows evaluation outcomes of the chaotic Rao-2 algorithm and a set of tactics mentioned in the literature. The assessment affirms the supremacy of the chaotic Rao-2 solver as well as its ability for large-scale frames. The model outcomes validate the scalability of the chaotic Rao-2 algorithm.

*6.2.2. Case 7: Reduction of Active Power Loss.* Real power loss reduction is as selected the objective to be achieved using the chaotic Rao-2 solver. Figure 10 shows the convergence trait obtained for this case. Figure 10 displays the advancement of the objective over iterations. The chaotic Rao-2 algorithm requires 85 iterations to get the optimal value, which demonstrates the excellent convergence rate of the chaotic Rao-2 algorithm when managing such a large-scale OPF formulation. The optimal solution achieved is given in Table 11. The real power loss is 36.483 MW. The model outcomes confirm the scalability of the chaotic Rao-2 algorithm.

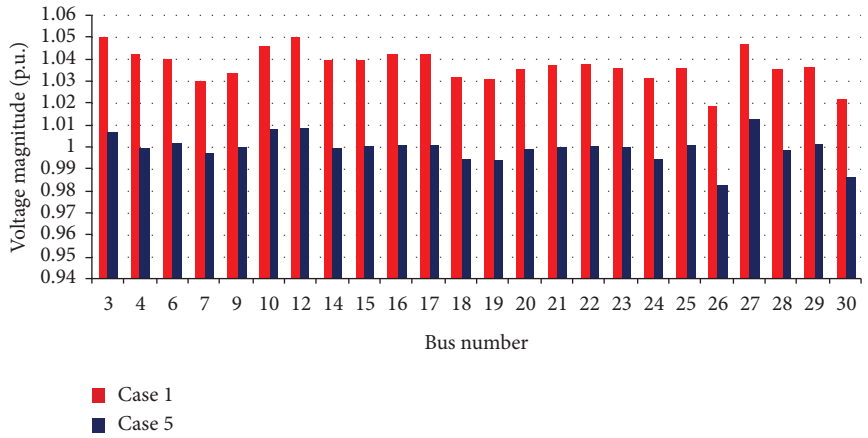


Figure 8: Comparison of the system voltage profile obtained for case 1 and case 5 using the chaotic Rao-2 algorithm.

Table 8: Statistical results obtained taking into account one hundred tests of the chaotic Rao-2 and the basic Rao-2 algorithms.

| Case | *Optimal value* | | *Worst value* | | *Mean value* | | *Standard deviation* | |
|---|---|---|---|---|---|---|---|---|
| | Chaotic Rao-2 | Basic Rao-2 | Chaotic Rao-2 | Basic Rao-2 | Chaotic Rao-2 | Basic Rao-2 | Chaotic Rao-2 | Basic Rao-2 |
| 1 | 800.1537 | 800.3865 | 800.2573 | 800.5841 | 800.1884 | 800.4395 | 0.0035 | 0.0048 |
| 2 | 3.0614 | 3.0975 | 3.0864 | 3.1363 | 3.0757 | 3.1164 | 0.0017 | 0.0023 |
| 3 | 0.12394 | 0.1243 | 0.12413 | 0.12469 | 0.12405 | 0.12451 | 0.00027 | 0.00033 |
| 4 | 0.0940385 | 0.103614 | 0.0972564 | 0.1183015 | 0.0957353 | 0.1086043 | 0.00014 | 0.00016 |

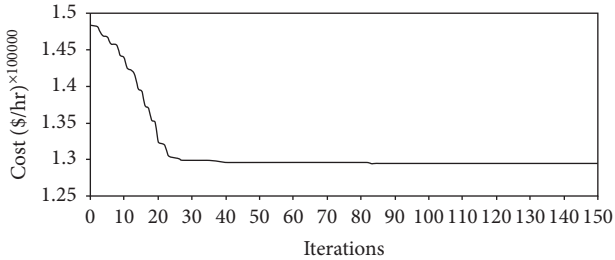


Figure 9: Convergence graph obtained for case 6 using the chaotic Rao-2 algorithm.

Table 9: Optimum solution obtained for case 6 using the chaotic Rao-2 algorithm.

| Item | Case 6 |
|---|---|
| $P_{G1}$ | 34.75893 |
| $P_{G4}$ | 0 |
| $P_{G6}$ | 0 |
| $P_{G8}$ | 0 |
| $P_{G10}$ | 398.50583 |
| $P_{G12}$ | 89.43075 |
| $P_{G15}$ | 24.72035 |
| $P_{G18}$ | 12.00462 |
| $P_{G19}$ | 18.01743 |
| $P_{G24}$ | 0.58246 |
| $P_{G25}$ | 184.05003 |
| $P_{G26}$ | 285.60488 |
| $P_{G27}$ | 9.84174 |
| $P_{G31}$ | 6.80405 |
| $P_{G32}$ | 18.63058 |
| $P_{G34}$ | 0.736515 |
| $P_{G36}$ | 6.40826 |
| $P_{G40}$ | 47.37403 |
| $P_{G42}$ | 45.63085 |
| $P_{G46}$ | 19.30682 |
| $P_{G49}$ | 215.47068 |
| $P_{G54}$ | 47.38042 |
| $P_{G55}$ | 26.30643 |
| $P_{G56}$ | 31.60362 |
| $P_{G59}$ | 154.73065 |
| $P_{G61}$ | 145.64302 |
| $P_{G62}$ | 0 |
| $P_{G65}$ | 364.30645 |
| $P_{G66}$ | 351.16057 |
| $P_{G69}$ | 453.27046 |
| $P_{G70}$ | 0 |
| $P_{G72}$ | 0 |
| $P_{G73}$ | 0 |
| $P_{G74}$ | 13.58035 |
| $P_{G76}$ | 18.51604 |
| $P_{G77}$ | 0 |
| $P_{G80}$ | 425.35715 |
| $P_{G85}$ | 0 |
| $P_{G87}$ | 5.31805 |
| $P_{G89}$ | 498.46802 |
| $P_{G90}$ | 0 |
| $P_{G91}$ | 0 |
| $P_{G92}$ | 0.82053 |
| $P_{G99}$ | 0 |
| $P_{G100}$ | 245.40568 |
| $P_{G103}$ | 38.48037 |
| $P_{G104}$ | 0 |
| $P_{G105}$ | 5.36204 |
| $P_{G107}$ | 28.73936 |
| $P_{G110}$ | 6.46135 |
| $P_{G111}$ | 26.35406 |
| $P_{G112}$ | 38.34864 |
| $P_{G113}$ | 0.53065 |
| $P_{G116}$ | 0 |
| $V_{G1}$ | 1.04153 |
| $V_{G4}$ | 1.06046 |
| $V_{G6}$ | 1.04803 |
| $V_{G8}$ | 1.08204 |
| $V_{G10}$ | 1.08525 |
| $V_{G12}$ | 1.04853 |
| $V_{G15}$ | 1.04196 |
| $V_{G18}$ | 1.05264 |
| $V_{G19}$ | 1.04362 |
| $V_{G24}$ | 1.06804 |
| $V_{G25}$ | 1.07163 |
| $V_{G26}$ | 1.08572 |
| $V_{G27}$ | 1.05403 |
| $V_{G31}$ | 1.03628 |
| $V_{G32}$ | 1.05216 |
| $V_{G34}$ | 1.06385 |
| $V_{G36}$ | 1.06253 |
| $V_{G40}$ | 1.05408 |
| $V_{G42}$ | 1.05174 |
| $V_{G46}$ | 1.05936 |
| $V_{G49}$ | 1.07328 |
| $V_{G54}$ | 1.05735 |
| $V_{G55}$ | 1.05819 |
| $V_{G56}$ | 1.05258 |
| $V_{G59}$ | 1.06526 |
| $V_{G61}$ | 1.08305 |
| $V_{G62}$ | 1.07326 |
| $V_{G65}$ | 1.08473 |
| $V_{G66}$ | 1.08427 |
| $V_{G69}$ | 1.09263 |
| $V_{G70}$ | 1.07594 |
| $V_{G72}$ | 1.06483 |
| $V_{G73}$ | 1.06512 |
| $V_{G74}$ | 1.05308 |
| $V_{G76}$ | 1.05103 |
| $V_{G77}$ | 1.08253 |
| $V_{G80}$ | 1.08642 |
| $V_{G85}$ | 1.08065 |
| $V_{G87}$ | 1.08316 |
| $V_{G89}$ | 1.08642 |
| $V_{G90}$ | 1.07314 |
| $V_{G91}$ | 1.07485 |
| $V_{G92}$ | 1.08153 |
| $V_{G99}$ | 1.08394 |
| $V_{G100}$ | 1.08685 |
| $V_{G103}$ | 1.08064 |
| $V_{G104}$ | 1.06835 |
| $V_{G105}$ | 1.06531 |
| $V_{G107}$ | 1.06384 |
| $V_{G110}$ | 1.07362 |
| $V_{G111}$ | 1.07253 |
| $V_{G112}$ | 1.05864 |
| $V_{G113}$ | 1.05242 |
| $V_{G116}$ | 1.08483 |
| $T_{8,5}$ | 1.03743 |
| $T_{26,25}$ | 1.07264 |
| $T_{30,17}$ | 1.05104 |
| $T_{38,37}$ | 0.98605 |
| $T_{63,59}$ | 1.03482 |
| $T_{64,61}$ | 0.98184 |
| $T_{65,66}$ | 0.97463 |
| $T_{68,69}$ | 0.95314 |
| $T_{81,80}$ | 1.02064 |
| $Q_{C34}$ | 23.6093 |
| $Q_{C44}$ | 3.9604 |
| $Q_{C45}$ | 23.6403 |

Table 9: Continued.

Table 9: Continued.

| Item | Case 6 |
|---|---|
| $Q_{C46}$ | 2.3182 |
| $Q_{C48}$ | 7.6316 |
| $Q_{C74}$ | 12.5934 |
| $Q_{C79}$ | 21.4703 |
| $Q_{C82}$ | 26.1483 |
| $Q_{C83}$ | 13.8403 |
| $Q_{C105}$ | 13.4174 |
| $Q_{C107}$ | 4.2745 |
| $Q_{C110}$ | 18.9753 |
| Loss (MW) | 75.05 |
| Cost ($/h) | 129,385.643 |
| CT (s) | 64.18 |
| No. of iterations | 83 |
| — | — |
| — | — |
| — | — |
| — | — |
| — | — |
| — | — |
| — | — |

The outcomes in intelligible form state optimum; $P_G$ (MW); $V_G$ (p.u.); $Q_C$ (Mvar).

Table 10: Comparison of solutions accomplished for case 6.

| Method | Cost ($/h) |
|---|---|
| ICBO [38] | 135,121.5704 |
| TLBO [41] | 129,682.844 |
| MSA [45] | 129,640.7191 |
| GPU-PSO [50] | 129,627.03 |
| MIB-EPSO-CO [51] | 130,288.21 |
| GWO [52] | 129,720 |
| IPM [53] | 129,720.70 |
| GSA [54] | 129,565 |
| COA [55] | 133,110.4316 |
| Chaotic Rao-2 | 129,385.643 |

The outcomes in intelligible form state optimum; NR, not reported.

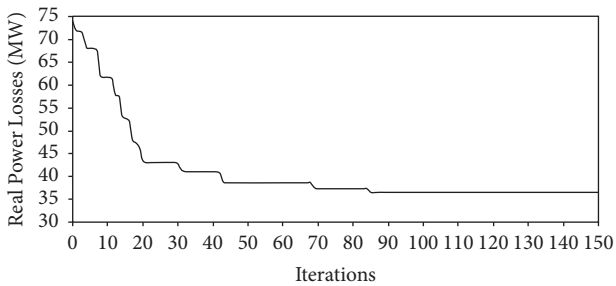


Figure 10: Convergence graph obtained for case 7 using the chaotic Rao-2 algorithm.

Table 11: Optimum solution obtained for case 7 using the chaotic Rao-2 algorithm.

| Item | Case 7 |
|---|---|
| $P_{G1}$ | 65.3683 |
| $P_{G4}$ | 14.538 |
| $P_{G6}$ | 34.1036 |
| $P_{G8}$ | 1.3604 |
| $P_{G10}$ | 196.4832 |
| $P_{G12}$ | 83.326 |
| $P_{G15}$ | 31.4628 |
| $P_{G18}$ | 70.4248 |
| $P_{G19}$ | 25.354 |
| $P_{G24}$ | 38.534 |
| $P_{G25}$ | 124.4852 |
| $P_{G26}$ | 215.5204 |
| $P_{G27}$ | 81.4832 |
| $P_{G31}$ | 63.0626 |
| $P_{G32}$ | 53.3065 |
| $P_{G34}$ | 48.4603 |
| $P_{G36}$ | 53.8951 |
| $P_{G40}$ | 86.5405 |
| $P_{G42}$ | 93.8039 |
| $P_{G46}$ | 94.964 |
| $P_{G49}$ | 153.4014 |
| $P_{G54}$ | 118.3516 |
| $P_{G55}$ | 65.9958 |
| $P_{G56}$ | 83.5034 |
| $P_{G59}$ | 158.1543 |
| $P_{G61}$ | 56.3842 |
| $P_{G62}$ | 24.5158 |
| $P_{G65}$ | 118.5032 |
| $P_{G66}$ | 215.6036 |
| $P_{G69}$ | 213.5152 |
| $P_{G70}$ | 15.3051 |
| $P_{G72}$ | 1.5816 |
| $P_{G73}$ | 38.0083 |
| $P_{G74}$ | 31.5813 |
| $P_{G76}$ | 40.7047 |
| $P_{G77}$ | 18.7493 |
| $P_{G80}$ | 451.463 |
| $P_{G85}$ | 3.538 |
| $P_{G87}$ | 4.6392 |
| $P_{G89}$ | 382.6042 |
| $P_{G90}$ | 65.8309 |
| $P_{G91}$ | 1.5302 |
| $P_{G92}$ | 1.572 |
| $P_{G99}$ | 1.473 |
| $P_{G100}$ | 174.6036 |
| $P_{G103}$ | 46.9537 |
| $P_{G104}$ | 13.5783 |
| $P_{G105}$ | 14.692 |
| $P_{G107}$ | 46.3064 |
| $P_{G110}$ | 19.426 |
| $P_{G111}$ | 35.4052 |
| $P_{G112}$ | 40.621 |
| $P_{G113}$ | 1.461 |
| $P_{G116}$ | 74.7025 |
| $V_{G1}$ | 1.0035 |
| $V_{G4}$ | 1.0363 |
| $V_{G6}$ | 1.0193 |
| $V_{G8}$ | 1.0482 |
| $V_{G10}$ | 1.0518 |

Table 11: Continued.

| Item | Case 7 |
|---|---|
| $V_{G12}$ | 1.0148 |
| $V_{G15}$ | 1.0036 |
| $V_{G18}$ | 1.0153 |
| $V_{G19}$ | 1.0012 |
| $V_{G24}$ | 1.0185 |
| $V_{G25}$ | 1.0428 |
| $V_{G26}$ | 1.0415 |
| $V_{G27}$ | 1.0016 |
| $V_{G31}$ | 1.0296 |
| $V_{G32}$ | 1.0091 |
| $V_{G34}$ | 1.0161 |
| $V_{G36}$ | 1.0052 |
| $V_{G40}$ | 1.0094 |
| $V_{G42}$ | 1.0068 |
| $V_{G46}$ | 1.0024 |
| $V_{G49}$ | 1.0382 |
| $V_{G54}$ | 1.0029 |
| $V_{G55}$ | 1.0013 |
| $V_{G56}$ | 0.9996 |
| $V_{G59}$ | 1.0054 |
| $V_{G61}$ | 0.9947 |
| $V_{G62}$ | 1.0012 |
| $V_{G65}$ | 1.0392 |
| $V_{G66}$ | 1.0175 |
| $V_{G69}$ | 1.0153 |
| $V_{G70}$ | 1.0018 |
| $V_{G72}$ | 1.014 |
| $V_{G73}$ | 1.0051 |
| $V_{G74}$ | 0.9905 |
| $V_{G76}$ | 0.9842 |
| $V_{G77}$ | 1.0013 |
| $V_{G80}$ | 1.0063 |
| $V_{G85}$ | 1.0027 |
| $V_{G87}$ | 1.0074 |
| $V_{G89}$ | 1.0153 |
| $V_{G90}$ | 1.0185 |
| $V_{G91}$ | 1.0012 |
| $V_{G92}$ | 1.0105 |
| $V_{G99}$ | 1.0026 |
| $V_{G100}$ | 1.0164 |
| $V_{G103}$ | 1.0053 |
| $V_{G104}$ | 0.995 |
| $V_{G105}$ | 1.0014 |
| $V_{G107}$ | 1.0174 |
| $V_{G110}$ | 1.0118 |
| $V_{G111}$ | 1.0225 |
| $V_{G112}$ | 1.0152 |
| $V_{G113}$ | 1.0297 |
| $V_{G116}$ | 1.0274 |
| $T_{8,5}$ | 1.0108 |
| $T_{26,25}$ | 1.0113 |
| $T_{30,17}$ | 1.0064 |
| $T_{38,37}$ | 1.0105 |
| $T_{63,59}$ | 1.0134 |
| $T_{64,61}$ | 1.0195 |
| $T_{65,66}$ | 1.0284 |
| $T_{68,69}$ | 1.0053 |
| $T_{81,80}$ | 1.0038 |
| $Q_{C34}$ | 23.8504 |
| $Q_{C44}$ | 18.8537 |
| $Q_{C45}$ | 19.7538 |
| $Q_{C46}$ | 10.8635 |
| $Q_{C48}$ | 20.7403 |
| $Q_{C74}$ | 13.9573 |
| $Q_{C79}$ | 21.768 |
| $Q_{C82}$ | 15.6239 |
| $Q_{C83}$ | 16.4052 |
| $Q_{C105}$ | 24.835 |
| $Q_{C107}$ | 15.8034 |
| $Q_{C110}$ | 13.864 |
| Loss (MW) | 36.483 |
| Cost ($/h) | 156,315 |
| CT (s) | 68.43 |
| No. of iterations | 85 |
| — | — |
| — | — |
| — | — |
| — | — |
| — | — |
| — | — |
| — | — |

The outcomes in intelligible form state optimum; $P_G$ (MW); $V_G$ (p.u.); $Q_C$ (Mvar).

## 7. Conclusions

This article reports the successful employment of a novel chaotic Rao-2 solver to solve the OPF framework in electrical power grids. A novel chaotic Rao-2 algorithm-inspired scheme for handling the OPF problem is offered. To handle the problem of premature convergence in the basic Rao-2 algorithm, the chaotic dynamic was amalgamated into the movement formula of the basic Rao-2 algorithm to enhance the variety of solutions and enhance both its global and local search capabilities. The liberation of the entrapped individuals in the local optima is possible because of a sudden alteration in the values offered by the chaotic oscillations. Unlike many other existing algorithms used to solve the OPF, the suggested chaotic Rao-2 algorithm does not need any algorithm-particular controlling parameters. Thus, the problem of premature convergence in the formerly reported techniques can be evaded. Furthermore, the chaotic Rao-2 algorithm involves an effective strategy to handle the state variable constraints to maintain the solution feasibility. Many population-based techniques offer an infeasible solution to the OPF problem in terms of violation of the state variable constraints because they are not supported by an efficient tactic to handle the state variable constraints. For scrutinizing the competence of the chaotic Rao-2 algorithm, it is examined on two typical IEEE test grids, considering five OPF cases. The studied cases are minimization of fuel cost, minimization of real power losses, voltage stability reinforcement, voltage profile improvement, and voltage profile improvement with cost reduction. The obtained results disclosed a set of main findings and conclusions. The simulation results demonstrate the robustness of the chaotic Rao-2 algorithm. Simulations revealed that the chaotic Rao-

2 algorithm is a fast-converging optimizer with good execution time. The chaotic Rao-2 algorithm outperforms the basic Rao-2 algorithm regarding convergence velocity and solution competence. In contrast to the basic Rao-2 algorithm, the attained computation times from the chaotic Rao-2 solver demonstrate that the suggested solver managed to converge to an optimal solution in less computation time than the basic Rao-2 algorithm for all of the studied cases. Due to its admirable exploration feature, the competitive computational time of the proposed algorithm makes it suitable for application in real power systems. The results of the chaotic Rao-2 are compared with other methods' results given in the former publications and found superior over other metaheuristic techniques to create valid as well as a global solution to OPF problems. The optimal values of fuel cost, real power losses, and voltage stability index identified with the chaotic Rao-2 algorithm are 800.1537 $/h, 3.0614 MW, and 0.12394, which are superior compared to the basic Rao-2 algorithm, and the former competitive optimization solvers reported in the literature. The chaotic Rao-2 algorithm is a competitive optimizer in terms of solution supremacy and computational time when solving the large-scale OPF problems. Furthermore, the statistical test stated that the chaotic Rao-2 solver is a trustworthy metaheuristic optimization tool in terms of exploration competence. In conclusion, it can be confirmed that the chaotic Rao-2 solver is a viable algorithm for solving various OPF frameworks. An optimal and feasible solution can be obtained by the chaotic Rao-2 algorithm. The simulation results confirm the scalability of the chaotic Rao-2 algorithm. In the future, the chaotic Rao-2 solver can be modified to solve multiobjective OPF problems. This algorithm can be used to solve the optimal reactive power flow problem.

## Data Availability

Data is available upon request from the author.

## Conflicts of Interest

The author declares that there are no conflicts of interest regarding the publication of this paper.

## References


[1] H. R. El-Hana Bouchekara, M. A. Abido, and A. E. Chaib, "Optimal power flow using an improved electromagnetism-like mechanism method," *Electric Power Components and Systems*, vol. 44, no. 4, pp. 434–449, 2016.

[2] B. Bentouati, M. S. Javaid, H. R. E. H. Bouchekara, and A. A. El-Fergany, "Optimizing performance attributes of electric power systems using chaotic salp swarm optimizer," *International Journal of Management Science and Engineering Management*, vol. 15, no. 3, pp. 165–175, 2020.

[3] S. Li, W. Gong, L. Wang, X. Yan, and C. Hu, "Optimal power flow by means of improved adaptive differential evolution," *Energy*, vol. 198, Article ID 117314, 2020.

[4] M. Kaur and N. Narang, "An integrated optimization technique for optimal power flow solution," *Soft Computing*, vol. 24, no. 14, pp. 10865–10882, 2020.

[5] K. Abaci and V. Yamacli, "Differential search algorithm for solving multi-objective optimal power flow problem," *International Journal of Electrical Power & Energy Systems*, vol. 79, pp. 1–10, 2016.

[6] J. C. Bansal, S. S. Jadon, R. Tiwari, D. Kiran, and B. K. Panigrahi, "Optimal power flow using artificial bee colony algorithm with global and local neighborhoods," *International Journal of System Assurance Engineering and Management*, vol. 8, no. S4, pp. 2158–2169, 2017.

[7] M. Basu, "Group search optimization for solution of different optimal power flow problems," *Electric Power Components and Systems*, vol. 44, no. 6, pp. 606–615, 2016.

[8] J. Ben Hmida, T. Chambers, and J. Lee, "Solving constrained optimal power flow with renewables using hybrid modified imperialist competitive algorithm and sequential quadratic programming," *Electric Power Systems Research*, vol. 177, Article ID 105989, 2019.

[9] A. A. El-Fergany and H. M. Hasanien, "Tree-seed algorithm for solving optimal power flow problem in large-scale power systems incorporating validations and comparisons," *Applied Soft Computing*, vol. 64, pp. 307–316, 2018.

[10] A. Mukherjee and V. Mukherjee, "Solution of optimal power flow using chaotic krill herd algorithm," *Chaos, Solitons & Fractals*, vol. 78, pp. 10–21, 2015.

[11] E. Naderi, M. Pourakbari-Kasmaei, and H. Abdi, "An efficient particle swarm optimization algorithm to solve optimal power flow problem integrated with FACTS devices," *Applied Soft Computing*, vol. 80, pp. 243–262, 2019.

[12] T. T. Nguyen, "A high performance social spider optimization algorithm for optimal power flow solution with single objective optimization," *Energy*, vol. 171, pp. 218–240, 2019.

[13] K. Pandiarajan and C. K. Babulal, "Fuzzy harmony search algorithm based optimal power flow for power system security enhancement," *International Journal of Electrical Power & Energy Systems*, vol. 78, pp. 72–79, 2016.

[14] I. N. Trivedi, P. Jangir, S. A. Parmar, and W. Meng, "Optimal power flow with enhancement of voltage stability and reduction of power loss using ant-lion optimizer," *Cogent Engineering*, vol. 3, no. 1, Article ID 1208942, 2016.

[15] R. V. Rao, "Rao algorithms: three metaphor-less simple algorithms for solving optimization problems," *International Journal of Industrial Engineering Computations*, vol. 11, pp. 107–130, 2020.

[16] D. Kumar and M. Rani, "Alternated superior chaotic variants of gravitational search algorithm for optimization problems," *Chaos, Solitons & Fractals*, vol. 159, Article ID 112152, 2022.

[17] A.-F. Attia, R. A. El Sehiemy, and H. M. Hasanien, "Optimal power flow solution in power systems using a novel Sine-Cosine algorithm," *International Journal of Electrical Power & Energy Systems*, vol. 99, pp. 331–343, 2018.

[18] M. Rezaei Adaryani and A. Karami, "Artificial bee colony algorithm for solving multi-objective optimal power flow problem," *International Journal of Electrical Power & Energy Systems*, vol. 53, pp. 219–230, 2013.

[19] S. Li, W. Gong, C. Hu, X. Yan, L. Wang, and Q. Gu, "Adaptive constraint differential evolution for optimal power flow," *Energy*, vol. 235, Article ID 121362, 2021.

[20] S. Abd el-sattar, S. Kamel, M. Ebeed, and F. Jurado, "An improved version of salp swarm algorithm for solving optimal power flow problem," *Soft Computing*, vol. 25, no. 5, pp. 4027–4052, 2021.

[21] A. Shaheen, A. Ginidi, R. El-Sehiemy, A. Elsayed, E. Elattar, and H. T. Dorrah, "Developed Gorilla troops technique for

optimal power flow problem in electrical power systems," *Mathematics*, vol. 10, p. 1636, 2022.

[22] S. P. Dash, K. R. Subhashini, and P. Chinta, "Development of a Boundary Assigned Animal Migration Optimization algorithm and its application to optimal power flow study," *Expert Systems with Applications*, vol. 200, Article ID 116776, 2022.

[23] Y. Li, Y. Li, G. Li, D. Zhao, and C. Chen, "Two-stage multi-objective OPF for AC/DC grids with VSC-HVDC: incorporating decisions analysis into optimization process," *Energy*, vol. 147, pp. 286–296, 2018.

[24] Y. Li and Y. Li, "Security-constrained multi-objective optimal power flow for a hybrid AC/VSC-mtdc system with lasso-based contingency filtering," *IEEE Access*, vol. 8, pp. 6801–6811, 2020.

[25] J. Hazra and A. K. Sinha, "A multi-objective optimal power flow using particle swarm optimization," *European Transactions on Electrical Power*, vol. 21, no. 1, pp. 1028–1045, 2011.

[26] E. Naderi, M. Pourakbari-Kasmaei, F. V. Cerna, and M. Lehtonen, "A novel hybrid self-adaptive heuristic algorithm to handle single- and multi-objective optimal power flow problems," *International Journal of Electrical Power & Energy Systems*, vol. 125, Article ID 106492, 2021.

[27] O. Akdag, "A improved Archimedes optimization algorithm for multi/single-objective optimal power flow," *Electric Power Systems Research*, vol. 206, Article ID 107796, 2022.

[28] M. Abbasi, E. Abbasi, and B. Mohammadi-Ivatloo, "Single and multi-objective optimal power flow using a new differential-based harmony search algorithm," *Journal of Ambient Intelligence and Humanized Computing*, vol. 12, no. 1, pp. 851–871, 2020.

[29] S. Gupta, N. Kumar, L. Srivastava, H. Malik, A. Anvari-Moghaddam, and F. P. García Márquez, "A robust optimization approach for optimal power flow solutions using Rao algorithms," *Energies*, vol. 14, no. 17, p. 5449, 2021.

[30] M. H. Hassan, S. Kamel, A. Selim, T. Khurshaid, and J. L. Domínguez-García, "A modified rao-2 algorithm for optimal power flow incorporating renewable energy sources," *Mathematics*, vol. 9, no. 13, p. 1532, 2021.

[31] I. Zelinka, Q. B. Diep, V. Snášel et al., "Impact of chaotic dynamics on the performance of metaheuristic optimization algorithms: an experimental analysis," *Information Sciences*, vol. 587, pp. 692–719, 2022.

[32] MATLAB, *Release R2018a*, The MathWorks, Inc, Natick, MA, USA, 2018.

[33] K. Y. Lee, Y. M. Park, and J. L. Ortiz, "A united approach to optimal real and reactive power dispatch," *IEEE Transactions on Power Apparatus and Systems*, vol. PAS-104, no. 5, pp. 1147–1153, 1985.

[34] R. A. El Sehiemy, F. Selim, B. Bentouati, and M. A. Abido, "A novel multi-objective hybrid particle swarm and salp optimization algorithm for technical-economical-environmental operation in power systems," *Energy*, vol. 193, Article ID 116817, 2020.

[35] S. Kumar and D. K. Chaturvedi, "Optimal power flow solution using GA-fuzzy and PSO-fuzzy," *Journal of the Institution of Engineers: Serie Bibliographique*, vol. 95, no. 4, pp. 363–368, 2014.

[36] S. S. Reddy, "Optimal power flow using hybrid differential evolution and harmony search algorithm," *International Journal of Machine Learning and Cybernetics*, vol. 10, no. 5, pp. 1077–1091, 2018.

[37] K. Teeparthi and D. M. Vinod Kumar, "Multi-objective hybrid PSO-APO algorithm based security constrained optimal power flow with wind and thermal generators," *Engineering Science and Technology, an International Journal*, vol. 20, no. 2, pp. 411–426, 2017.

[38] H. R. E. H. Bouchekara, A. E. Chaib, M. A. Abido, and R. A. El-Sehiemy, "Optimal power flow using an improved colliding bodies optimization algorithm," *Applied Soft Computing*, vol. 42, pp. 119–131, 2016.

[39] A. Ramesh Kumar and L. Premalatha, "Optimal power flow for a deregulated power system using adaptive real coded biogeography-based optimization," *International Journal of Electrical Power & Energy Systems*, vol. 73, pp. 393–399, 2015.

[40] P. P. Biswas, P. N. Suganthan, R. Mallipeddi, and G. A. J. Amaratunga, "Optimal power flow solutions using differential evolution algorithm integrated with effective constraint handling techniques," *Engineering Applications of Artificial Intelligence*, vol. 68, pp. 81–100, 2018.

[41] H. R. E. H. Bouchekara, M. A. Abido, and M. Boucherma, "Optimal power flow using Teaching-Learning-Based Optimization technique," *Electric Power Systems Research*, vol. 114, pp. 49–59, 2014.

[42] A. A. Abou El Ela, M. A. Abido, and S. R. Spea, "Optimal power flow using differential evolution algorithm," *Electric Power Systems Research*, vol. 80, no. 7, pp. 878–885, 2010.

[43] A.-F. Attia, Y. A. Al-Turki, and A. M. Abusorrah, "Optimal power flow using adapted genetic algorithm with adjusting population size," *Electric Power Components and Systems*, vol. 40, no. 11, pp. 1285–1299, 2012.

[44] S. Duman, U. Güvenç, Y. Sönmez, and N. Yörükeren, "Optimal power flow using gravitational search algorithm," *Energy Conversion and Management*, vol. 59, pp. 86–95, 2012.

[45] A.-A. A. Mohamed, Y. S. Mohamed, A. A. M. El-Gaafary, and A. M. Hemeida, "Optimal power flow using moth swarm algorithm," *Electric Power Systems Research*, vol. 142, pp. 190–206, 2017.

[46] M. S. Kumari and S. Maheswarapu, "Enhanced genetic algorithm based computation technique for multi-objective optimal power flow solution," *International Journal of Electrical Power & Energy Systems*, vol. 32, no. 6, pp. 736–742, 2010.

[47] A. Bhattacharya and P. K. Chattopadhyay, "Application of biogeography-based optimisation to solve different optimal power flow problems," *IET Generation*, Transmission & Distribution, vol. 5, pp. 70–80, 2011.

[48] A. Ananthi Christy and P. A. D. Vimal Raj, "Adaptive biogeography based predator–prey optimization technique for optimal power flow," *International Journal of Electrical Power & Energy Systems*, vol. 62, pp. 344–352, 2014.

[49] I. Pena, C. B. Martinez-Anido, and B. M. Hodge, "The IEEE 118-bus test system," vol. 33, 1962, https://ieeexplore.ieee.org/xpl/RecentIssue.jsp?punumber=59http://www.ee.washington.edu/%20research/pstca/pg_tca118bus.html.

[50] V. Roberge, M. Tarbouchi, and F. Okou, "Optimal power flow based on parallel metaheuristics for graphics processing units," *Electric Power Systems Research*, vol. 140, pp. 344–353, November 2016.

[51] V. H. Hinojosa and R. Araya, "Modeling a mixed-integer-binary small-population evolutionary particle swarm algorithm for solving the optimal power flow problem in electric power systems," *Applied Soft Computing*, vol. 13, no. 9, pp. 3839–3852, September 2013.

[52] A. A. El-Fergany and H. M. Hasanien, "Single and multi-objective optimal power flow using grey wolf optimizer and differential evolution algorithms," *Electric Power Components and Systems*, vol. 43, no. 13, pp. 1548–1559, July 2015.

[53] Q. Jiang, G. Geng, C. Guo, and Y. Cao, "An efficient implementation of automatic differentiation in interior point optimal power flow," *IEEE Transactions on Power Systems*, vol. 25, no. 1, pp. 147–155, 2010.

[54] A. Bhattacharya and P. K. Roy, "Solution of multi-objective optimal power flow using gravitational search algorithm," *IET Generation*, Transmission & Distribution, vol. 6, pp. 751–763, 2012.

[55] T. N. L. Anh, D. N. Vo, W. Ongsakul, P. Vasant, and T. Ganesan, "Cuckoo optimization algorithm for optimal power flow," in *Proceedings of the 18th Asia Pacific Symposium on Intelligent and Evolutionary Systems*, vol. 1, pp. 479–493, Springer, Heidelberg, Germany, 2015.